Multiscale Upscaling Study for CO_2 Storage in Carbonate Rocks Using Machine Learning and Multiscale Imaging

Yong, Wen Pin; Menke, Hannah; Maes, Julien; Geiger, Sebastian; Bakar, Zainol Affendi Abu; Lewis, Helen; Buckman, Jim; Bonnin, Anne; Singh, Kamaljit

DOI
10.4043/34892-MS

Publication date
2024

Document Version
Final published version

Published in
Offshore Technology Conference Asia, OTCA 2024

OTC-34892-MS

Multiscale Upscaling Study for CO_2 Storage in Carbonate Rocks Using Machine Learning and Multiscale Imaging

Wen Pin Yong, PETRONAS Research Sdn. Bhd., Bangi, Malaysia; Hannah Menke and Julien Maes, Institute of GeoEnergy Engineering, Heriot-Watt University, Edinburgh, United Kingdom; Sebastian Geiger, Department of Geoscience and Engineering, Delft University of Technology, Delft, Netherlands; Zainol Affendi Abu Bakar, PETRONAS Research Sdn. Bhd., Bangi, Malaysia; Helen Lewis and Jim Buckman, Institute of GeoEnergy Engineering, Heriot-Watt University, Edinburgh, United Kingdom; Anne Bonnin, Paul Scherrer Institut, Swiss Light Source, Villigen PSI, Switzerland; Kamaljit Singh, Institute of GeoEnergy Engineering, Heriot-Watt University, Edinburgh, United Kingdom

This paper was prepared for presentation at the Offshore Technology Conference Asia held in Kuala Lumpur, Malaysia, 27 February - 01 March 2024.

Abstract

Microporosity is commonly assumed to be non-connected porosity and not commonly studied in geoengineering industry. However, the presence of micropores plays a key role in connecting macropores and it can contribute significantly to the overall flow performance. In this study, targeted CO_2 storage carbonate fields in Southeast Asia have significant amounts of microporosity ranging from 10 to 60% of the total measured porosity. Microporosity can only be seen in high resolution images. To study the unresolved and the resolved microporosity, Middle Miocene carbonate samples from CO_2 storage candidate fields were scanned using lower resolution micro-computed micro-tomography (micro-CT) and higher resolution synchrotron light source to understand the pore scale structure of the carbonate sample at different length scales. This paper proposes a proof-of-concept upscaling method that integrates multiscale 3D imaging techniques and trendline analysis to establish porosity-permeability relationships with microporosity insight. After image acquisition and processing, the images were divided into smaller sub-volumes. Pore-scale modelling was conducted to predict the permeability using Darcy-Brinkman-Stokes (DBS) model. Then, a nano-scale porosity-permeability transform is generated using natural log trendline fitting based on simulation results. The porosity-permeability transform is further extended to three cases to cover the low case, mid case, and high case of datapoint fittings and is further validated with laboratory measured data. The established porosity-permeability transforms in this study have been applied to compare with petrophysical derived porosity-permeability transforms with better performance (higher R^2 value) for low permeability datapoint. The multiscale imaging upscaling workflow has integrated machine learning during image segmentation with pore-scale modelling and trendline fitting during the upscaling study. It emphasises the importance of seeing the unseen (unresolved microporous phase) to understand the

internal texture and microstructure of a rock sample in order to understand the connectivity of the overall flow performance in a carbonate rock.

Introduction

Carbonate rocks are complex with multiple length scales and multiple scales of heterogeneity. The complexity is contributed to secondary porosity developed during diagenesis. These rocks have multiple Representative Elementary Volumes (REV) for different sample sizes, and it is challenging to establish porosity-permeability relationships that are valid at different measurement scales (submillimetre to decametre scales) [1]. For example, porosity can be measured directly using gas expansion at centimeter-scale in a core plug and indirectly at decimeter scale using subsurface wireline logs. The integration of these measurements at different length scales is still uncertain.

During reservoir characterisation, porosity that stands for the pore spaces in reservoir system, and permeability that stands for the ability of flow in porous media, are the main properties to govern CO_2 storage and petroleum production field development. The interconnectivity in carbonate rocks is mainly contributed by micropores and macropores. Micropores are important contributors to connect the pathway between microporous grains and macropores [2]. These micropores refer to small pores that are present inside carbonate grains, matrix and cement which normally appears as unresolved phase under thin section and low-resolution micro-CT imaging tomograph. To solve the mystery of the unresolved phase, Middle Miocene carbonate rock samples from potential CO_2 storage depleting gas fields have been analysed using high- and low-resolution 3D imaging tomography. The studied location is a carbonate play locating at offshore Malaysia (Figure 1) and developed during Early to Middle Miocene.

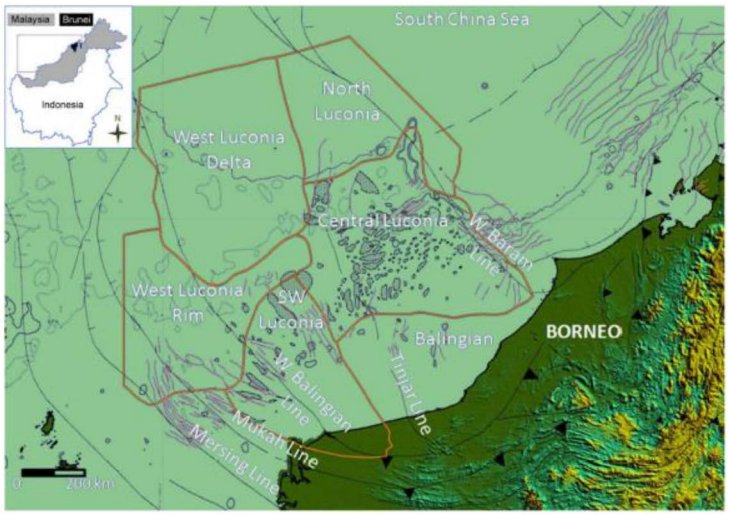

Figure 1—The studied Middle Miocene carbonate play at offshore Malaysia [6]

Cantrell and Hagerty [2] studied Arab formation carbonates of Saudi Arabia and they observed the microporosity forming process transforms different grain types into grains that have similar internal fabrics using high resolution SEM (Scanning Electron Microscope) equipment. Janjuhah [6] and Habibur [7] observed a significant amount of microporosity in the same carbonate play for this study. They compared the visible porosity from 2D petrographic thin sections to the total porosity measured by routine core analysis (RCA) to estimate the amount of microporosity in samples. Both literature studies quantified the amount of microporosity based on 2D imaging technique with a thin slice of rock with only 30 microns thickness. To enhance the microporosity study for complex carbonate rocks, we proposed a multiscale imaging study

using 3D image analysis, pore-scale modelling, and multiscale upscaling study as more representative way of quantifying microporosity under multiple length of scales (nano-scale, micro-scale, and core-scale).

Methods

In this study, the workflow consists of six main stages (Figure 2). Middle Miocene carbonate rock samples from potential CO_2 storage depleting gas fields were selected and plugged in core warehouse. A total of seven cylindrical shape carbonate rocks with 38.1 mm diameter and 52.07-73.66 mm length were selected based on different lithofacies, pore types, porosity, and permeability range (Figure 3). The sample information is summarised in Table 1. Sample A was selected for multiscale imaging. During sample preparation, sample A core was drilled for micro-scale imaging study and the subplug sample is laser-cut for nano-scale imaging using Oxford Laser service.

Table 1—The information of selected carbonate samples

Sample ID	Porosity, %	Permeability, m^2	Diameter (mm)	Length (mm)	Classification
Sample A	37.05	1.1547×10^{-14}	38.1	73.66	Mouldic limestone
Sample B	30.72	2.1351×10^{-13}	38.1	62.23	Framestone
Sample C	31.66	9.9211×10^{-14}	38.1	52.07	Floatstone
Sample D	29.55	9.0747×10^{-14}	38.1	60.96	Bindstone
Sample E	32.98	2.2631×10^{-13}	38.1	60.96	Rudstone
Sample F	27.50	1.7402×10^{-13}	38.1	53.34	Bafflestone
Sample G	31.93	1.1633×10^{-13}	38.1	73.66	Packstone

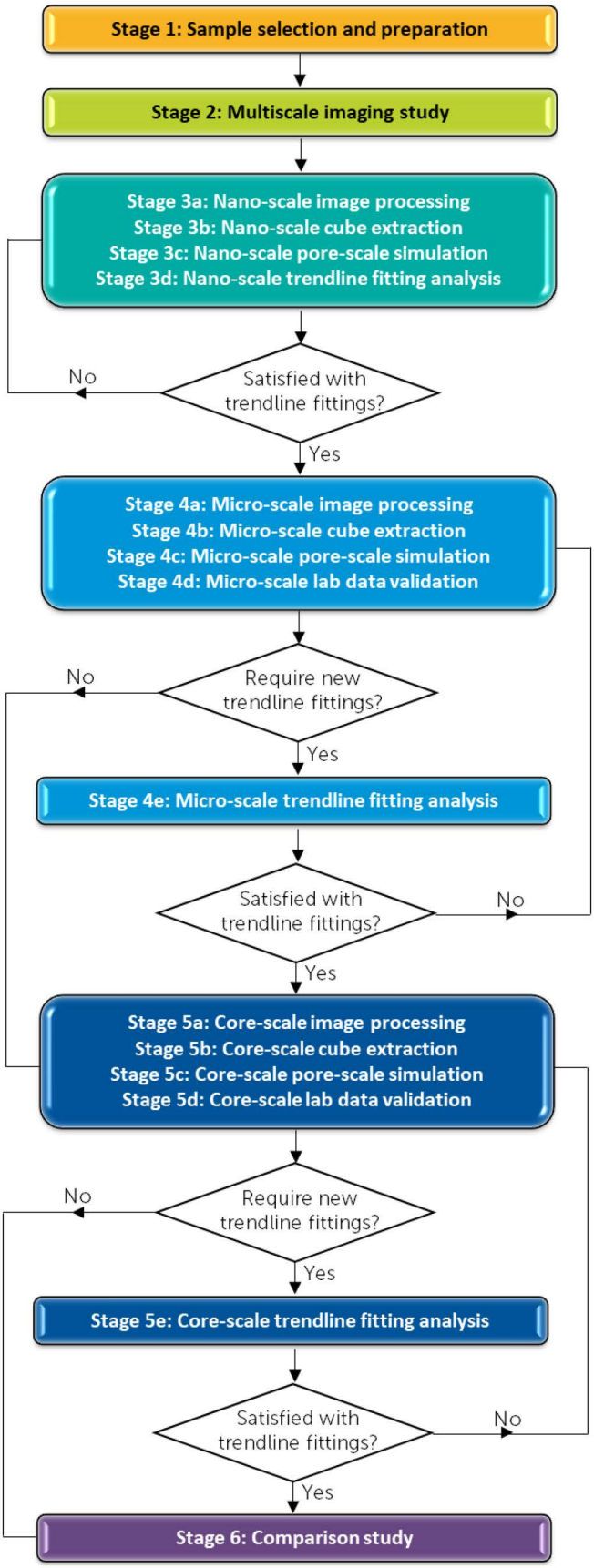

Figure 2—The workflow for this study

Figure 3—Selected carbonate core samples (38.1mm diameter) in this study

Multiscale imaging study was conducted using Rx Solutions EasyTom micro-CT and Swiss Light Source (SLS) Tomographic Microscopy Coherent rAdiology experimenTs (TOMCAT) beamline synchrotron radiation facility at PSI (Paul Scherrer Institut), Villigen, Switzerland. The imaging study starts with core-scale imaging using micro-CT equipment at 22.5 µm voxel size (38.1 mm cylindrical shape core sample), followed by micro-scale imaging using micro-CT equipment at 5.5 µm voxel size (6 mm cylindrical shape subplug sample), and finally nano-scale imaging using SLS TOMCAT at 0.165 µm voxel size (500 µm cylindrical shape mini plug sample). Figure 4 shows the acquired images during multiscale imaging study.

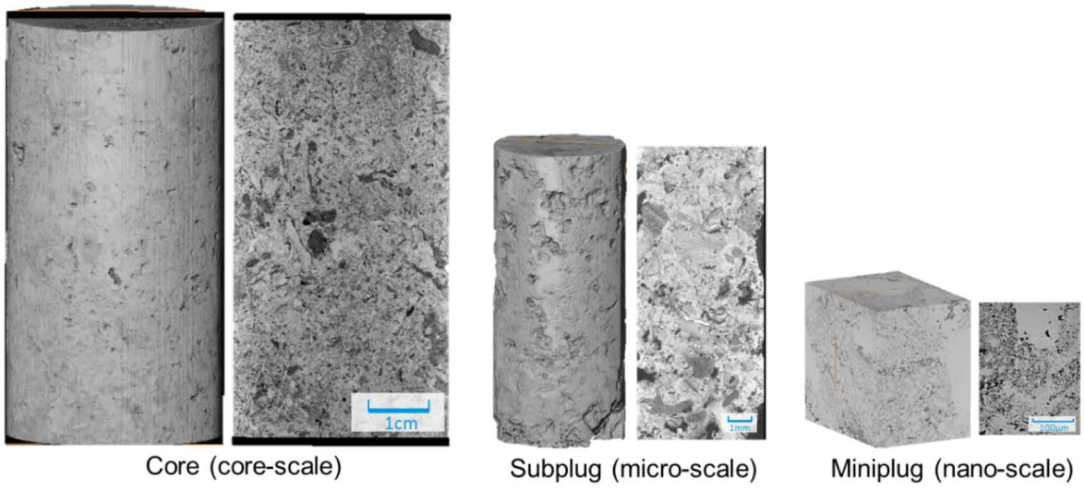

Figure 4—Multiscale imaging data from 3D dataset

The image datasets were first processed by volume editing to remove the surrounding of sample; cropped to remain the volume of interest; filtered to remove image noise and segmented to separate different phases (pore, solid and/or microporous phase) in the sample. In this study, nano-scale image dataset was segmented into pore and solid phases (binary image); micro-scale image dataset was segmented into three phases (pore, solid and/or microporous phase) and core-scale was not segmented but converted to 255-phases greyscale image dataset (Figure 5). Avizo software was used for most of the image processing steps except micro-scale three phase segmentation that was performed using 3D Weka (Waikato Environment for Knowledge Analysis) machine learning based segmentation using ImageJ software [8].

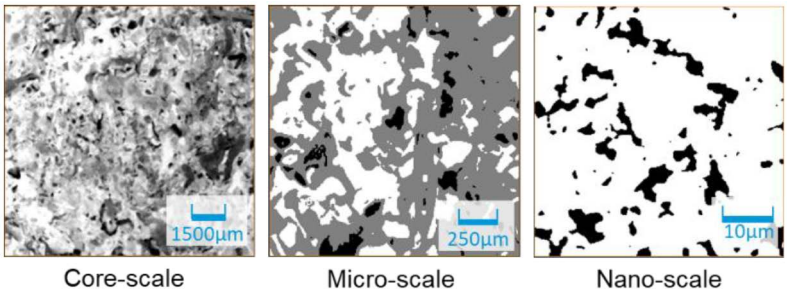

Figure 5—Multiscale imaging data after image processing

After image processing, pore-scale simulation was conducted to find out the connected porosity and flow streamlines (permeability). During the simulation, the image dataset was divided into smaller 300×300×300 voxel cubic size images to generate more datapoints and avoid simulation crash (Figure 6). For nano-scale simulation, simpleFoam solver was used to compute the flow in the pore space using constant velocity and fluid viscosity. For micro-scale simulation, simpleDBSFoam was used to solve DBS equation [9]. The porosity in microporous phase was calculated based on mean value of greyscale intensity divided by total greyscale intensity while the permeability in microporous phase was calculated based on nano-scale trendline fitting equation. For core-scale simulation, simpleDBSFoam was used as well and individual porosity and permeability values were assigned to 255 phases of image dataset. GeoChemFoam software was used for pore-scale simulation. This open source OpenFoam CFD (Computational Fluid Dynamics) toolbox software is developed at the Institute of GeoEnergy Engineering, Heriot-Watt University [10].

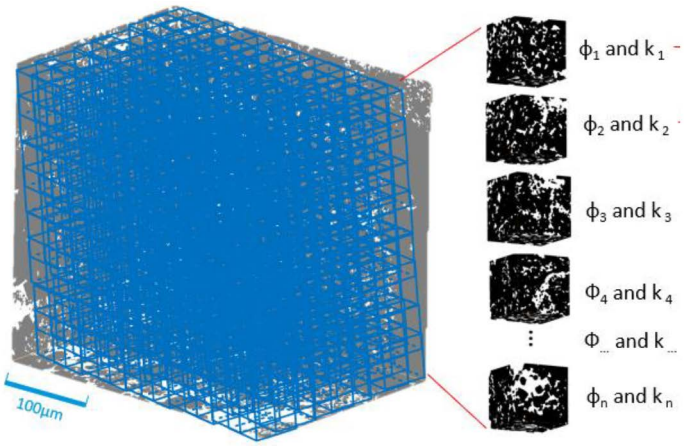

Figure 6—Cubes extraction into 300 × 300 × 300 voxel sizes

Multiscale upscaling study started from nano-scale pore-scale simulation results. It is important to have nano-scale imaging dataset to allow a clear identification between pore and solid phases in the internal fabrics and microstructure or resolved features. Nano-scale permeability and porosity results were plotted and regressed for trendline analysis. In this study, three nano-scale trendline fitting equations were generated to represent low case, mid case, and high case. These equations were then used to define the permeability in microporous phase during micro-scale simulation study.

For micro-scale image dataset, the lower resolution consists of microporous phase with unresolved porosity which cannot be visualised in lower resolution images and requires image segmentation into three or more phases. During image segmentation, it is not straightforward to segment the studied phases using conventional thresholding segmentation method because it is less accurate or misses details in segmentation result. Therefore, machine learning based 3D Weka segmentation method based on pixel-based was applied using a set of selected image features from machine learning algorithms. A freehand selection tool of 1

pixel width was used to draw out the identified phases separately before training the classifier for the whole image. Figure 7 compares the segmentation results based on thresholding segmentation (Figure 7b) and machine learning (Figure 7c). It is observed that thresholding segmentation result produces less pore spaces (black colour phase) compared to machine learning segmentation, which are highlighted in blue circles.

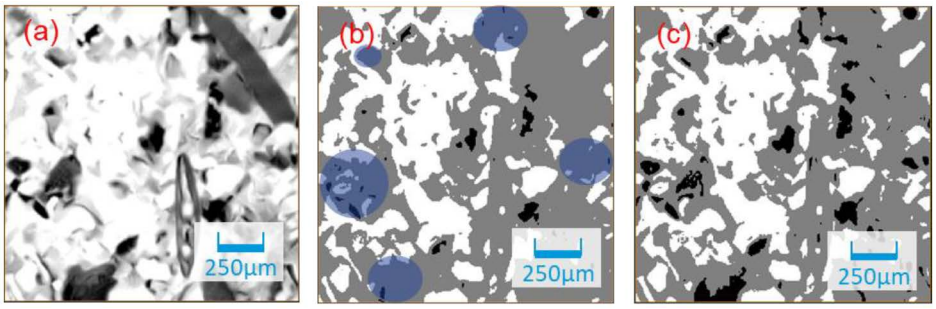

Figure 7—Image segmentation results, (a) greyscale image; (b) thresholding segmentation and (c) machine learning basis segmentation

Subplug laboratory measurement from flow experiment was used to validate the performance of trendline fitting equation. Micro-scale permeability and porosity results were then plotted and micro-scale trendline fitting analysis might need to be performed if the laboratory data and simulation results did not match the trendline fitting. Core sample laboratory measurement from Coreval 700 porosity permeability measurement equipment was used to validate the performance of trendline fitting equation. In this study, MATLAB software curve fitting tool was used to perform trendline fittings and graph plotting. The final generated trendline fitting equations were used to predict the permeability at core scale and compared with petrophysical derived porosity-permeability equations.

Results and Discussion

Nano-scale simulation results (connected porosity and permeability) were plotted in graph for trendline fitting analysis using curve fitting method. In this study, 1542 porosity and permeability data points from three directions were combined and trendlines were fitted using different equation types (linear, exponential, polynomial, power law and natural log). Among the fitting types, exponential, polynomial, power law, and natural log trendline fittings showed better fitting performance with R^2 value greater than 0.75. Those fittings were plotted in Figure 8. It is observed that most of the trendline fittings overpredicted the permeability especially porosity value beyond 0.3 except natural log fitting. Therefore, natural log fitting type was selected for the next simulation scale.

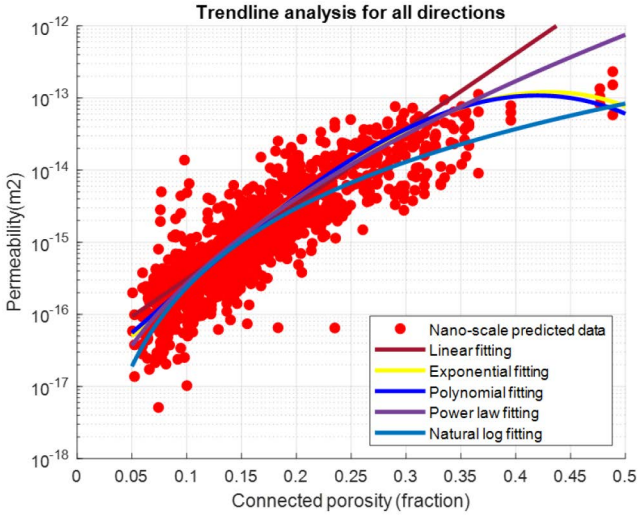

Figure 8—Nano-scale trendline fitting analysis

There are a wide range of porosity (0.05 - 0.48) and permeability (5.11×10^{-18} - 2.32×10^{-13}) values from nano-scale simulation. In order to have more representative trendline fitting trend, two additional natural log fitting trendlines were added to cover the upper range and lower range of permeability data. The new fittings were generated using high permeability and low permeability datapoints separately. Figure 9 shows the three natural log fitting equations or porosity-permeability transforms from nano-scale imaging study. The natural log fitting trendlines are expressed as,

Low case: Permeability (m^2) = 8.106×10^{-13} × porosity (fraction)$^{4.3575}$
Mid case: Permeability (m^2) = 1.048×10^{-12} × porosity (fraction)$^{3.645}$
High case: Permeability (m^2) = 3.013×10^{-12} × porosity (fraction)$^{3.226}$

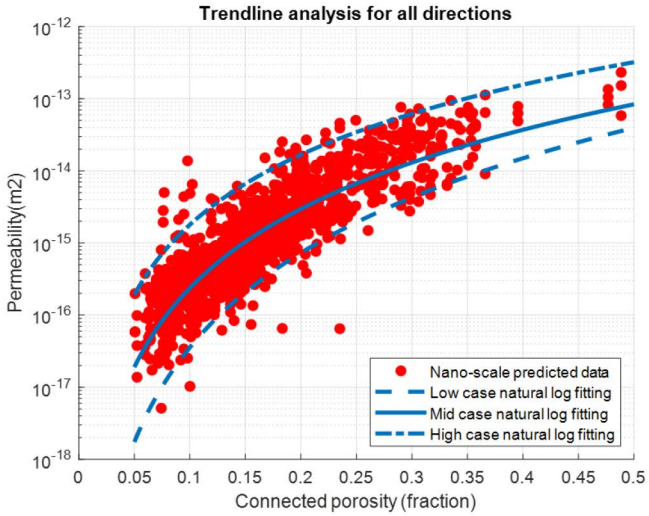

Figure 9—Natural log trendline fittings for nano-scale data

Micro-scale simulations were conducted based on natural log trendline fitting and validated with subplug laboratory measurements. In this case, the mid case natural log fitting equation was applied to calculate the permeability in microporous phase because the subplug lab data has the closest matching with mid case fitting (green points in Figure 10). Figure 10 shows the matching of simulation results and laboratory measurement with respect to natural log trendline fitting. Mid case natural log trendline can fit lab measured

data very well. At the same time, mid case natural log fitting can match the micro-scale simulation results quite well with less than one order of magnitude difference and R^2 value equals to 0.7962.

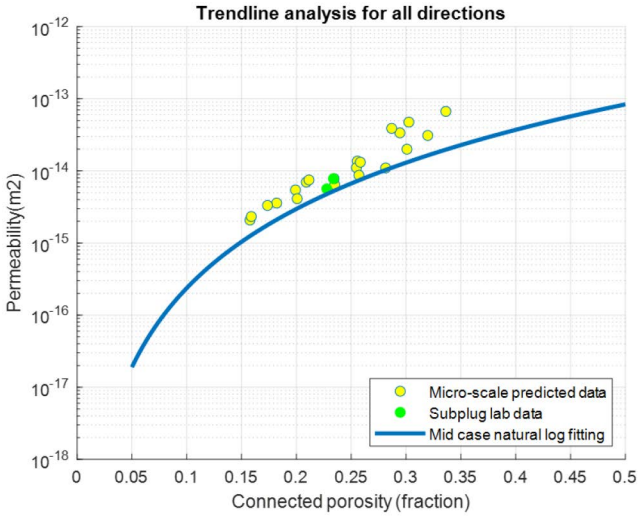

Figure 10—Micro-scale trendline fitting analysis

Core-scale simulations were conducted based on nano-scale trendline fitting since the micro-scale fitting was good. Low case natural log trendline fitting was applied to define the permeability in 253 phases of microporous phase (excluding pore phase and solid phase) because the core sample lab data has the closest matching with low case fitting (blue point in Figure 11). During core-scale simulation, 255-phase segmentation instead of 3-phase segmentation was applied due to the presence of high microporous phase volume (as high as 0.9 volume fraction) in core-scale images. The simulation results were validated with core sample laboratory measurement. Figure 11 shows the comparison of simulation results and laboratory measurement with respect to natural log trendline fitting. Low case natural log trendline can fit lab measured data very well and it can match the core-scale simulation results quite well with less than one order of magnitude difference and R^2 value equals to 0.8901.

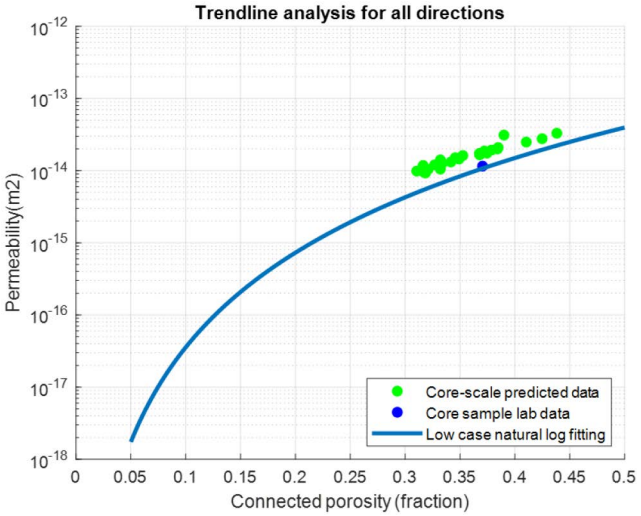

Figure 11—Core-scale trendline fitting analysis

There is a good matching between the natural log trendline fittings with micro-scale and core-scale simulation results. To prove the performance of the newly developed porosity-permeability transforms,

a comparison study was made between petrophysical derived and imaging derived porosity-permeability transforms in this study. Porosity-permeability transforms were normally derived based on different petrophysical rock typing methods such as porosity range, zone location, lithofacies, depositional environment, rock texture and combination of different facies. In this study, Dunham's carbonate rock texture classification was applied to classify the studied samples. Each rock type has its own power law derived porosity-permeability equation and it is common that one field will have more than three rock typing equations.

On the other hand, our imaging derived equations consist of only three equations. During comparison study, laboratory porosity and permeability measurements from the selected samples were first plotted together with natural log trendline fittings to select the nearest fitting to be applied. Among the samples, Sample A is different from the other carbonate samples because the sample was selected from different field and it has high porosity and low permeability properties. Based on the plot in Figure 12, low case natural log trendline fitting was applied to sample A while high case natural log trendline fitting was applied for the rest of the studied carbonate samples.

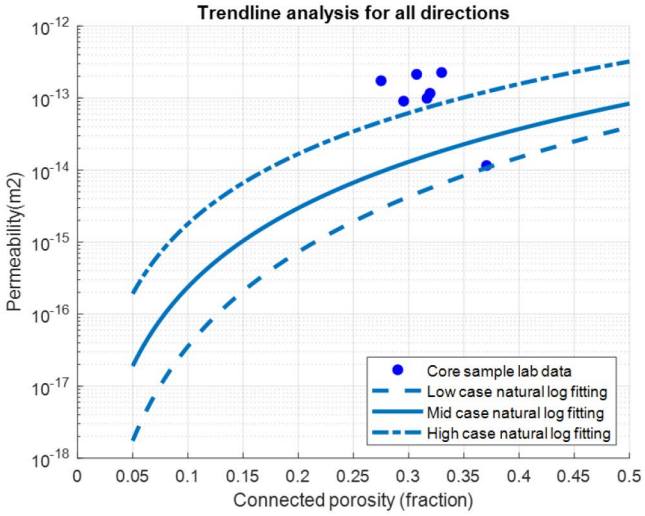

Figure 12—Trendline fitting selection for studied carbonate samples

Table 2 shows the permeability prediction results for petrophysical derived method and imaging derived method. Based on error analysis, the petrophysical derived method has a low R^2 value (0.0465). The method cannot handle high porosity sample with low permeability value (Sample A) accurately. On the other hand, our imaging derived method is better than petrophysical derived method with higher R^2 value (0.4479). The above study shows a 3D imaging workflow which integrates multiscale (nano-scale, micro-scale and core-scale) imaging information to study the porosity-permeability relationship. It highlights the importance of capturing microstructure details at nano-scale using high resolution imaging tool to understand the unresolved microporous phase in micro-scale and core-scale.

Table 2—Comparison study between petrophysical derived and imaging derived permeability

Sample ID	Core-scale lab measured porosity (fraction)	Core-scale lab measured permeability (m^2)	Petrophysical derived permeability (m^2)	Imaging derived permeability (m^2)	Petrophysical derived method
Sample A	0.37	1.1547×10^{-14}	3.2626×10^{-13}	1.0710×10^{-14}	Porosity range
Sample B	0.31	2.1351×10^{-13}	4.2919×10^{-13}	6.6937×10^{-14}	Framestone
Sample C	0.32	9.9211×10^{-14}	9.9687×10^{-14}	7.3764×10^{-14}	Floatstone
Sample D	0.30	9.0747×10^{-14}	1.8341×10^{-13}	5.9031×10^{-14}	Bindstone
Sample E	0.33	2.2631×10^{-13}	2.9203×10^{-13}	8.4186×10^{-14}	Rudstone
Sample F	0.28	1.7402×10^{-13}	9.3753×10^{-14}	4.6811×10^{-14}	Bafflestone
Sample G	0.32	1.1633×10^{-13}	8.0554×10^{-14}	7.5828×10^{-14}	Packstone

Conclusion

Measuring porosity and permeability at one scale (core-scale) is insufficient to derive representative and robust porosity-permeability relationships for carbonate rocks. This study investigated the microporosity in carbonate samples at multiple length scales. A multiscale upscaling workflow was developed based on multiscale imaging, multiscale upscaling, and pore-scale simulation. Porosity-permeability transforms based on microporosity insight were derived and compared with petrophysical derived porosity-permeability equations. The imaging method has the capability of predicting high porosity carbonate samples with low permeability value. Further work is needed to improve the study. It is recommended to add more imaging datasets and improve the trendline fittings using random upscaling or multiplication factor in upcoming study.

Acknowledgement

We acknowledge PETRONAS for allowing us to publish this work and the Paul Scherrer Institut, Villigen, Switzerland for provision of synchrotron radiation beamtime at beamline TOMCAT of the SLS and technical support.

References

1. P. W. M. Corbett, "Petroleum geoengineering: Integration of static and dynamic models: SEG/EAGE Distinguished Instructor Series, 12," SEG, p. 100p, 2009.
2. D. L. Cantrell and R. M. Hagerty, "Microporosity in Arab Formation Carbonates, Saudi Arabia," *GeoArabia*, vol. **4**, no. 2, pp. 129–154, 1999.
3. E. D. Pittman, "Microporosity in carbonate rocks," *Am. Assoc. Pet. Geol. Bull.*, vol. **55**, no. 10, pp. 1873–1881, 1971.
4. G. T. Baechle, A. Colpaert, G.P. Eberli, and R.J. Weger, "Effects of microporosity on sonic velocity in carbonate rocks," *Lead. Edge*, vol. **27**, pp. 1012–1018, 2008, doi: 10.7588/worllitetoda.89.5.0034.
5. R. J. Weger, G. P. Eberli, G.T. Baechle, J.L. Massaferro, and Y.F. Sun, "Quantification of pore structure and its effect on sonic velocity and permeability in carbonates," *Am. Assoc. Pet. Geol. Bull.*, vol. **93**, no. 10, pp. 1297–1317, 2009, doi: 10.1306/05270909001.
6. H. T. Janjuhah, A. Mohammad, A. Salim, A. Alansari, and D.P. Ghosh, "Presence of microporosity in Miocene carbonate platform, Central Luconia, offshore Sarawak, Malaysia," 2018.

7. R. Md Habibur, B. J. Pierson, and K. K. Ting, "A review of porosity classification in carbonates: challenges in Miocene reservoirs of Central Luconia, offshore Sarawak, Malaysia," in International Conference on Integrated Petroleum Engineering and Geosciences (ICIPEG), 2012.
8. Image, J., "Trainable Weka Segmentation," 2023. [Online]. Available: https://imagej.net/plugins/tws/. [Assessed: 27 November 2023].
9. H. C. Brinkman, "A calculation of the viscous force exerted by a flowing fluid on a dense swarm of particles," *Appl. Sci. Res*., vol. **1**, pp. 27–34, 1949.
10. J. Maes and H. P. Menke, "A Bespoke OpenFOAM Toolbox for Multiphysics Flow Simulations in Pore Structures," in 17th International Conference on Flow Dynamics. ICFD2020, 2020.